HYPER EXPERIMENTS ON CATASTROPHIC HYDROGEN RELEASES INSIDE A FUEL CELL ENCLOSURE

Friedrich, A., Kotchourko, N., Stern, G., and Veser, A.
Pro-Science GmbH, Parkstrasse 9, Ettlingen, 76275, Germany, *surname*@pro-science.de

ABSTRACT

As a part of the experimental work of the EC-funded project HYPER Pro-Science GmbH performed experiments to evaluate the hazard potential of a severe hydrogen leakage inside a fuel cell cabinet. During this study hydrogen distribution and combustion experiments were performed using a generic enclosure model with the dimensions of the fuel cell "Penta H2" provided by ARCOTRONICS (now EXERGY Fuel Cells) to the project partner UNIPI for their experiments on small foreseeable leaks. Hydrogen amounts of 1.5 to 15 g H_2 were released within one second into the enclosure through a nozzle with an internal diameter of 8 mm. In the distribution experiments the effects of different venting characteristics and different amounts of internal enclosure obstruction on the hydrogen concentrations measured at fixed positions in- and outside the model were investigated. Based on the results of these experiments combustion experiments with ignition positions in- and outside the enclosure and two different ignition times were performed. BOS (Background-Oriented-Schlieren) observation combined with pressure and light emission measurements were performed to describe the characteristics and the hazard potential of the induced hydrogen combustions. The experiments provide new experimental data on the distribution and combustion behaviour of hydrogen that is released into a partly vented and partly obstructed enclosure with different venting characteristics.

1.0 INTRODUCTION

Due to the increasing importance of hydrogen as an energy carrier it is necessary to investigate hazards arising from its use, especially in small scale applications designed for domestic use. The experiments described in this paper were performed in the frame of the EC funded project HYPER, which was investigating hazards arising from small stationary hydrogen and fuel cell applications to formulate an Installation Permitting Guidance document (IPG) for such devices. This document now allows a fast track approval of safety and procedural issues and provides a comprehensive agreed installation permitting process for developers, design engineers, manufacturers, installers and authorities having jurisdiction across the European Union. The present work was part of the experimental program and covered the scenarios C and D on catastrophic releases. In more than 200 experiments the hazard potential of a severe hydrogen leakage inside a fuel cell cabinet was comprehensively investigated. Furthermore, the experimental findings provided a trustworthy data basis for the validation of modelling and simulation work performed for risk evaluation.

2.0 EXPERIMENTAL SETUP

2.1 Enclosure geometry

All experiments were conducted with an enclosure model of the dimensions 700 x 800 x 1000 mm (internal volume: 560 l) that was installed in the hydrogen test chamber of the IKET (Institute for Nuclear and Energy Technologies) at the Forschungszentrum Karlsruhe (FZK, Karlsruhe Research Centre). Three cases distinguished by different venting characteristics of the enclosure model were investigated. In case 1 the enclosure was equipped with two vent openings arranged diagonally on two opposite walls. In this configuration passive (blue rectangles in the left part of Fig. 1) and active venting by two additional fans (small magenta squares with arrows in the left part of Fig. 1) was investigated. In case 2 the model was equipped with enlarged vent openings of doubled size (Fig. 1, centre), while in case 3 again the small vent openings were used, but an additional chimney was mounted to the top of the enclosure. Only passive venting was investigated in the cases 2 and 3.

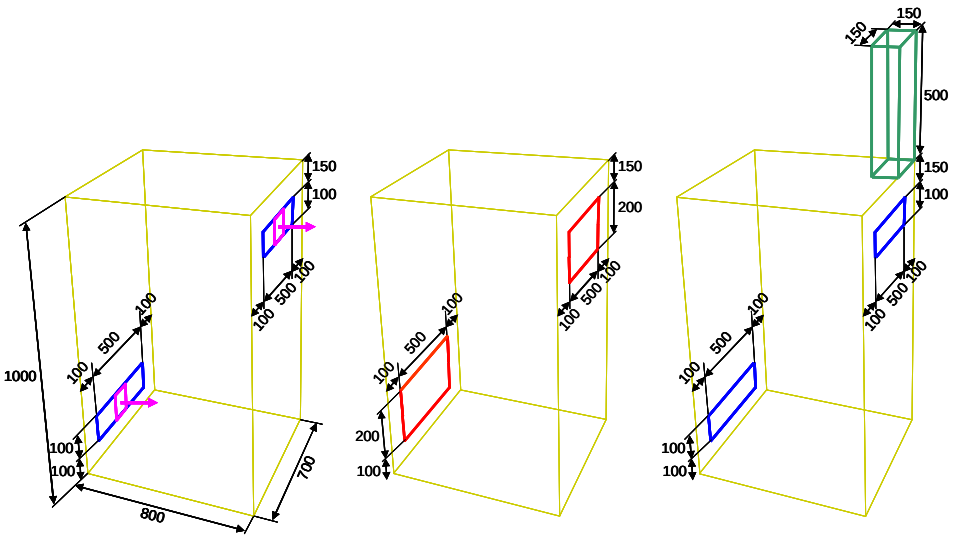

Figure 1: Sketch of the three venting characteristics (cases) investigated in the experiments.

Fig. 2 shows the two different internal geometries that were used in the distribution experiments. In these geometries the internals of a fuel cell are represented by obstacles with different blockage ratios. A solid cube at the bottom of the enclosure represents large solid components, while smaller ones such as wires, pipes and the like are represented by grids with a blockage ratio of 50%. Apart from facilitating both experimental and computational work, this simplification was made to generate three homogeneous but different areas inside the enclosure which can also occur in real fuel cell enclosures: completely blocked regions, areas with no obstruction and areas with partial obstruction. The latter is of particular interest for hydrogen safety studies, since combustions in obstructed areas have high potential for flame acceleration and even for detonation onset.

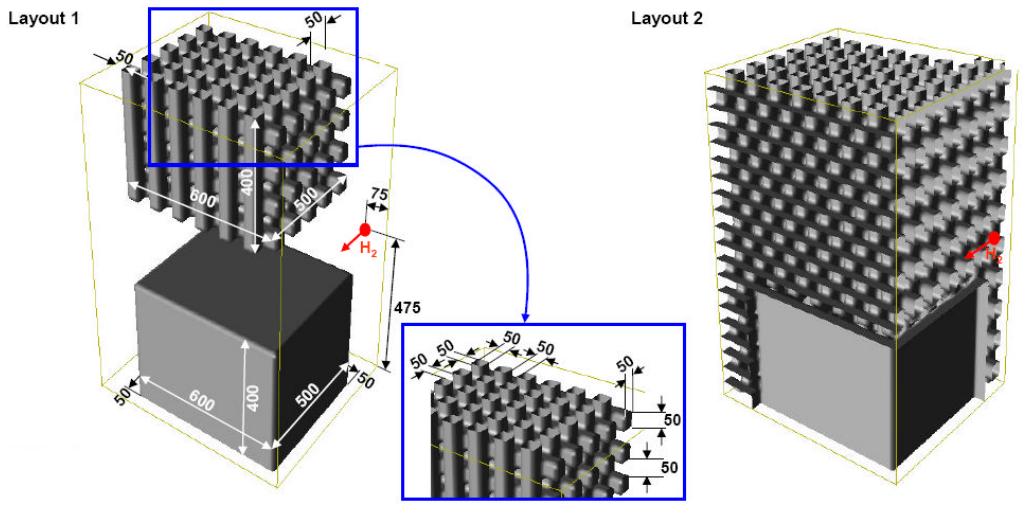

Figure 2: Internal geometry of the enclosure model for the experiments with low (left) and high obstruction (right).

In both internal geometries the size and position of the solid cube obstacle on the bottom of the enclosure remained unchanged. For the remaining free space two internal geometries were investigated. In the experiments with low obstruction of the internal enclosure volume a grid cube obstacle was mounted below its lid (see Fig. 2, left). In this configuration about 32% of the internal

volume of the enclosure is occupied by the obstacles (gas volume inside the enclosure approx. 380 l), which is close to the amount of blocked volume in the fuel cell that was used as a prototype for the experimental setup. In the experiments with high obstruction (Fig. 2, right) the entire free space inside the enclosure is occupied by grids with the same characteristics as the one used for the grid cube obstacle in the low obstructed geometry, reducing the gas volume inside the enclosure to approx. 240 l. In this configuration approx. 57% of the internal volume is occupied by the obstacles.

2.2 Hydrogen release system

Hydrogen was released horizontally into the enclosure through a nozzle with an internal diameter of 8 mm located perpendicular to its rear wall, as it is shown in the left part of Fig. 2. The position and direction of the nozzle remained unchanged in all experiments. Based on the description of a commercially available fuel cell unit the maximum hydrogen release rate possible in the case of a rupture of the hydrogen feed line inside the enclosure was evaluated to 15 gH_2/s, so in the experiments hydrogen release rates of 1.5 to 15 gH_2/s were used. In the scenario investigated an additional safety mechanism is assumed to shut down the H_2-supply after 1 s due to the pressure decrease inside the fuel cell system. To provide a constant H_2-mass flow with a defined duration a suitable hydrogen release system was constructed. A sketch of this hydrogen release system is depicted in Fig. 3.

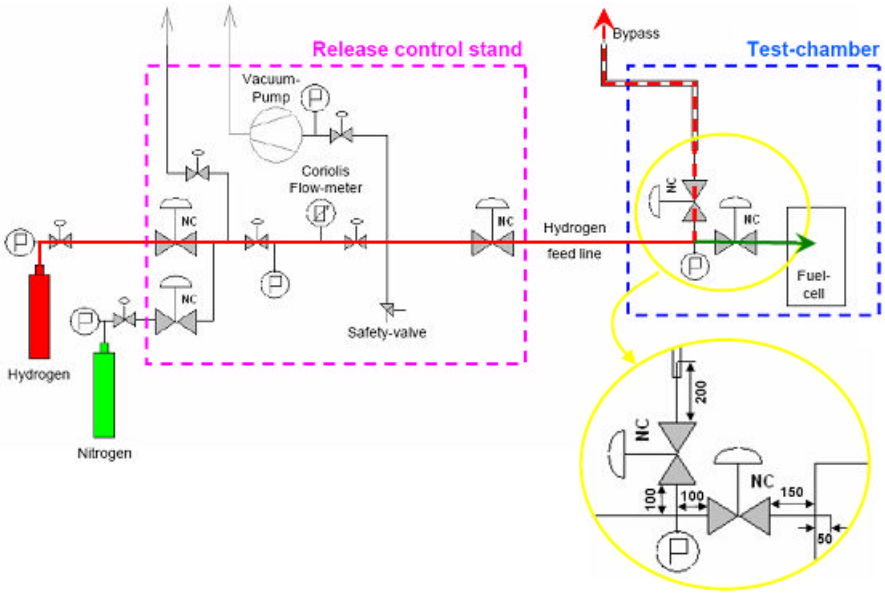

Figure 3: Sketch of the hydrogen release system used in the experiments.

Hydrogen (Quality 5.0) from storage cylinders was conducted through pipes to the release control stand, from where it was piped into the test chamber with the model of the fuel cell enclosure. Inside the test chamber the hydrogen line branched into a bypass and a release line with the same flow characteristics (see yellow highlighted part of Fig. 3). The hydrogen flow rate was adjusted in the release control stand while the hydrogen was piped through the bypass line to the ambience (dashed red arrow in Fig. 3). When the desired flow rate was reached bypass and release valve were switched simultaneously computer controlled to conduct the flow into the enclosure (green arrow in Fig. 3). After 1 s both valves were switched to bypass flow again computer controlled. Due to the conversion of the electrical signal provided by the control computer into a pneumatic signal for the valves the real hydrogen injection lasted from 0.1 to 1.1 s after an experiment was started. The hydrogen release properties were monitored and recorded by three devices in every experiment. The correct H_2-flow was adjusted via a Coriolis flow meter in the release control stand, a Prandtl-Probe was installed to the bypass line and a pressure sensor (Model JUMO pTrans p30) was located in the junction of release

and bypass line. With the signals recorded it is possible to determine the H_2-flow through the nozzle and the opening time of the release valve for all experiments. The measured opening times in the experiments varied in a range from 1 s ± 30 ms (average 994 ms) with an averaged injection time from 0.104 s to 1.098 s after an experiment was started. The H_2-mass flow was adjusted to the desired value with an accuracy of ± 0.4% in all experiments.

3.0 RESULTS

3.1 Distribution experiments

In total more than 120 distribution experiments with different release rates were performed on the cases described above. In these experiments H_2-concentrations were measured in- and outside the enclosure model at fixed times after the beginning of an experiment. The concentration measurements were performed by analysing gas samples that were taken via computer controlled sample taking cylinders (STCs). The STCs had a volume of approx. 300 ml and were equipped with two ports that were closed by electrical valves that allow remote opening. The inlet valve was equipped with a cannula (d_i = 2 mm, l = 500 mm) that was pointing to the gas sampling point, while the other valve, used for the evacuation of the cylinder prior to an experiment, was equipped with a self sealing coupling. The STCs required an opening time of their inlet valve of 2 s to be filled to an internal pressure that allowed the subsequent determination of the H_2-concentration. The gas samples were analysed using a gas analysing system (Fisher-Rosemount, Series MLT) with a measuring range from 0 to 100 vol.% H_2 and a measuring uncertainty of ≤ 1% FS. Experiments with the following five sampling periods after the beginning of an experiment were performed: 0.2 – 2.2 s, 2.0 – 4.0 s, 4.0 – 6.0 s, 6.0 – 8.0 s and 30 – 32 s. Eight STCs with the same opening period were used in every experiment. The positions of most of the STCs remained unchanged throughout all experiments with low obstruction, but changes in the positions of two STCs were necessary due to the different cases to be investigated and measurements in additional positions. The left part of Fig. 4 shows the experimental facility with the sampling positions in most of the experiments with low obstruction. In addition to the concentration measurements the distribution behaviour of the released hydrogen was monitored using BOS (Background-Oriented-Schlieren) photography, an optical method for the visualization of density gradients (Fig. 4, right).

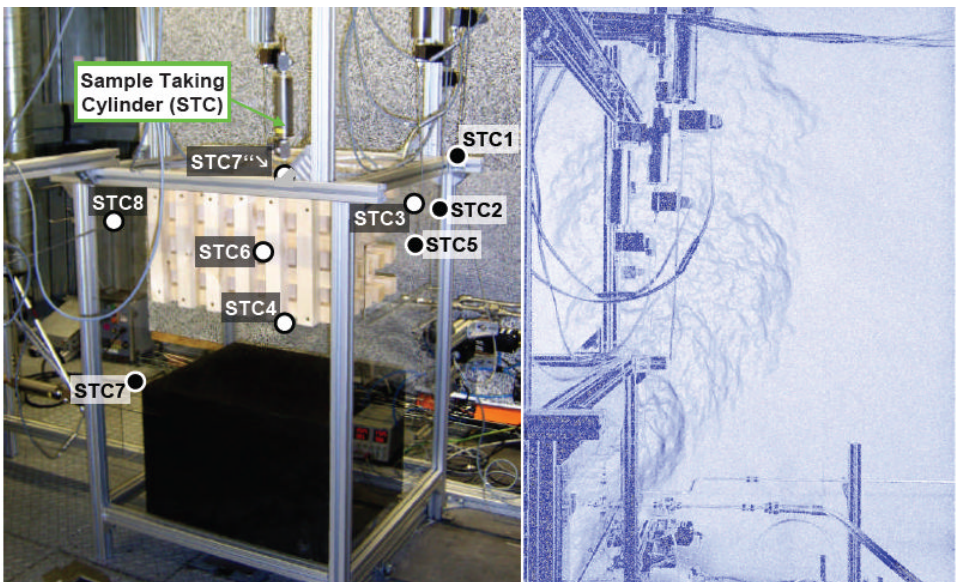

Figure 4: Sampling positions in the distribution experiments with low obstruction (left, white or black dots represent sampling positions in- or outside the enclosure) and BOS-photograph of the upper vent opening in a distribution experiment on case 2 with a released H_2-amount of 6 g.

Low obstruction: Due to the buoyancy of the released hydrogen forced ventilation (so called chimney effect) was observed in all experiments with the low obstructed internal geometry. In this configuration the lower vent opening acted as inlet for the fresh air, while the upper one was the exit for the H_2/air mixture generated inside the enclosure during the hydrogen release, as the BOS-photograph of the upper vent opening, depicted in the right part of Fig. 4, shows. In the experiments on case 3 the additional chimney took the role of the upper vent opening. Due to this effect only in the first sampling period (0.2 – 2.2 s) significant hydrogen concentrations were measured close to the lower vent opening of the enclosure (STC7). In most of the other sampling positions in- and outside the enclosure model the highest hydrogen concentrations were measured in the two sampling periods between 2.0 and 6.0 s, and in most of the experiments the highest concentrations inside the enclosure were measured by the STCs 3 and 8, located close to the rear and front wall. The concentrations in the centre of the grid cube (STC6) and in the centre of the enclosure (STC4) were lower. Compared to case 1a the distribution inside the enclosure is more homogeneous in all other cases, and compared to case 1a a faster transport of the released hydrogen to the outside of the enclosure was observed in the cases 1b (active venting) and 3 (additional chimney). H_2-concentrations above the flame acceleration limit were detected 30 s after its injection in the additional STC-position 7" shortly below the centre of the lid in the cases 1a and 2, while considerably lower H_2-concentrations were found after the same time for case 1b (7 vol.%) and especially for case 3 (5 vol.%).

High obstruction: In the experiments with the highly obstructed internal geometry the chimney effect described above was not observed, and compared to the experiments with low obstruction outside the enclosure only small H_2-concentrations were measured. At the same time inside it an inhomogeneous mixture distribution with very high hydrogen concentrations close to the walls and beneath the top was observed. Due to the high H_2-concentrations found inside the enclosure model in the distribution experiments with the highly obstructed internal geometry it was decided not to perform combustion experiments with such internal geometry.

The results of the evaluation of the concentration measurements concerning release rates leading to concentrations above the flammability (4 vol.%H_2) and the flame acceleration limit (10 vol.%H_2) as well as release rates producing concentrations close to the stoichiometric composition (~30 vol.%H_2) of H_2/air-mixtures in- and outside the enclosure for all cases are summarised in Table 1.

Table 1: Release rates leading to H_2-concentrations higher than 4 and 10 vol.%, and close to 30 vol.% in- and outside the enclosure model for experiments with low and high obstruction (Release time: 1 s).

	H_2-concentration inside the enclosure model			H_2-concentration outside the enclosure model		
	> 4 vol.%	> 10 vol.%	~ 30 vol.%	> 4 vol.%	> 10 vol.%	~ 30 vol.%
Case	Release rates [g H_2/s]			Release rates [g H_2/s]		
Low Obstruction						
1a	≥ 1.5	≥ 5	15	≥ 3	≥ 10	-
1b	≥ 3	≥ 4	15	≥ 3	≥ 5	15
2	≥ 3	≥ 5	15	≥ 3	≥ 6	-
3	≥ 3	≥ 4	15	≥ 3*	≥ 4*	15*
High Obstruction						
1a	≥ 1.5	≥ 3	≥ 6	≥ 4	10	-
1b	≥ 1.5	≥ 3	≥ 6	≥ 6	-	-

*in the additional Position 2' above the chimney

The values listed in Table 1 demonstrate that for the low obstructed enclosure model even with a released H_2-amount of 3 g flammable atmospheres in- and outside the enclosure are generated. H_2-concentrations close to the stoichiometric composition were found inside the low obstructed model after the release of 15 g H_2. Outside the enclosure released H_2-amounts of 15 g evoked concentrations close to the stoichiometric composition in case 1b. In case 3 H_2-concentrations similar to the ones measured inside the enclosure were measured in the additional sampling position above the chimney (Position 2'), while the concentrations determined close to the upper vent opening are significantly

lower than in all other cases. In the experiments with the highly obstructed geometry flammable H_2-concentrations were detected even after the release of 1.5 g H_2, and concentrations far above the flame acceleration limit after the injection of 3 g H_2. The release of 6 g H_2 already produced hydrogen concentrations close to the stoichiometric composition of H_2/air-mixtures, and maximum concentrations of more than 40 vol.% H_2 were measured close to the walls inside the enclosure after the release of 10 g H_2 in the two cases investigated.

3.2 Combustion experiments

Using the results of the distribution experiments the test matrix for the combustion experiments was established. Due to the high H_2-concentrations measured inside the highly obstructed enclosure model it was decided not to perform combustion experiments in this configuration.

In the combustion experiments two scenarios differed by the location of the ignition position were investigated. In the experiments on scenario C an ignition position inside the enclosure was used, that was located on the front wall close to the main switch ("CMS" in Fig. 5) of the prototype fuel cell. In scenario D outside ignition positions, located close to the upper rim of the upper vent opening ("OUT" in Fig. 5, all cases) or in an additional position above the centre of the chimney ("EXT" in Fig. 5, only case 3) were employed. Additionally two different ignition times were used in the experiments. A delayed ignition, where the ignition source was turned on 4 s after an experiment was started (duration 300 ms), was chosen since in the distribution experiments the highest H_2-concentrations were observed most often in the sampling periods between 2.0 and 6.0 s, and a permanent ignition, where the ignition source was turned on simultaneously with the start of the experiment for a duration of 5 s, to account for ignition sources that are permanently present, as, for instance, a hot surface. As ignition source a stable current and high voltage discharge at 60 kV with a frequency of 20 kHz between two electrodes (distance: ~ 5 mm) was used to produce spark discharges with energies from 10 to 20 W.

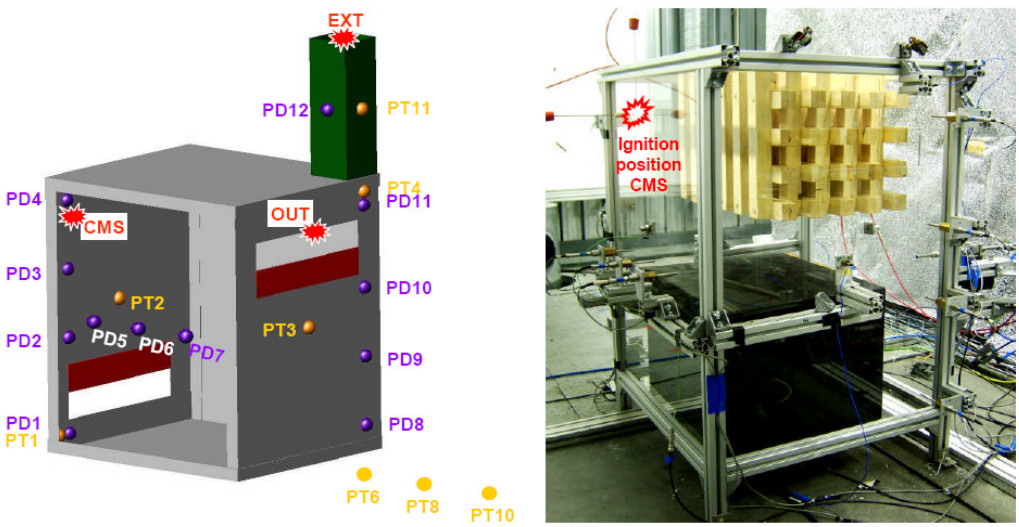

Figure 5: Sketch of the ignition and sensor positions used in the combustion experiments (left) and photograph of the enclosure model before an experiment on scenario C for case 2 (right).

In the combustion experiments pressure measurements were performed using ten piezoelectric sensors (yellow dots labelled PT in the left part of Fig. 5). Four of these sensors were positioned close to the edges and the centres of the sidewalls of the enclosure, while the remaining six pressure sensors were arranged in two lines on the floor besides the vent openings (the line besides the left vent opening consisting of PT5, PT7, and PT9 is not depicted in Fig. 5; its sensor positions are similar to the ones of PT6, PT8, and PT10). Eleven photodiodes (purple dots labelled PD in the left part of Fig. 5), arranged in two vertical lines close to the front and rear wall, and one horizontal line at half height of the front

wall were used to determine the position of the flame front. In the experiments on case 3 two additional sensors (PT11 and PD12) were installed to the chimney.

In total 35 experiments were performed on scenario C with the ignition source in position CMS. In 38 of 45 experiments on scenario D the ignition position OUT was used, while in the remaining 7 experiments the ignition source was located in position EXT above the centre of the chimney. Although it was planned to concentrate on combustion experiments with H_2-amounts of up to 6 g, two additional experiments with higher hydrogen inventories were performed. In the first of these experiments 14.85 g H_2 were released within approx. 2.5 s and ignited delayed after 4 s in position OUT (facility in configuration for case 2). In the second additional experiment on case 1a 23.41 g H_2, released within 3.9 s, were ignited delayed after 4 seconds in the same ignition position. Both additional experiments completely destroyed the enclosure model.

In many experiments with low hydrogen amounts none of the sensors or only few sensors positioned close to the top of the enclosure recorded indications for a combustion. In some of the corresponding BOS-photographs that were taken during the experiments a regional combustion was observed that quenched after some time without propagating through the whole enclosure. Fig. 6 shows two examples for this behaviour.

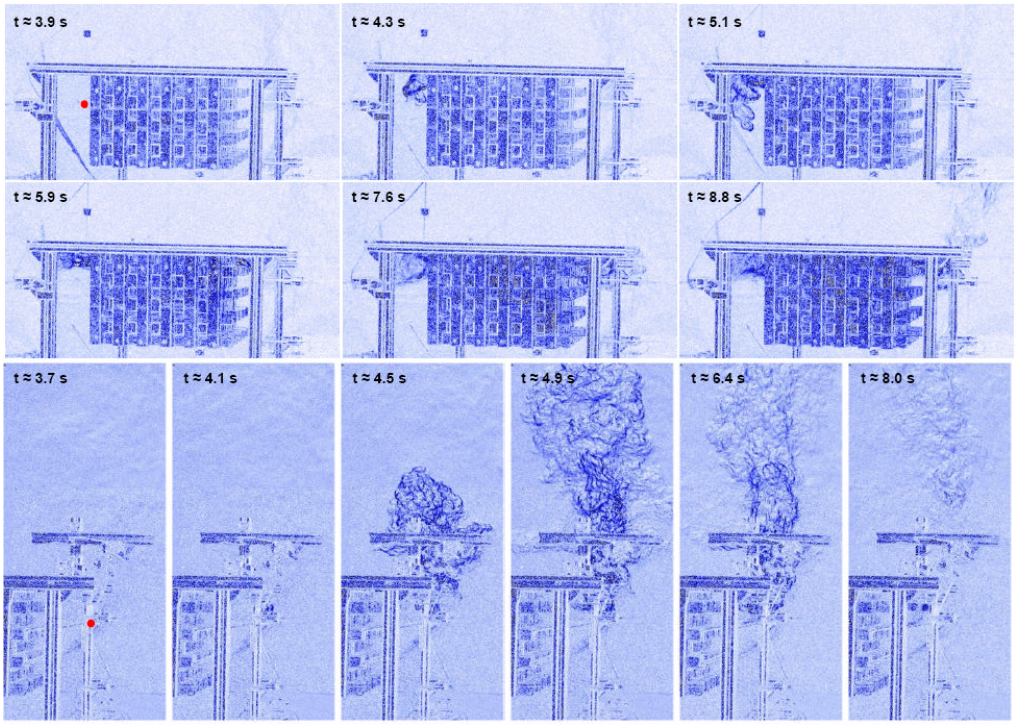

Figure 6: BOS-photos of experiments with regional combustion after delayed ignition in position CMS (upper part: case 2, 1.5 g H_2) and OUT (lower part: case 1a, 3 g H_2) after 4 s. The red dot in the first frames of both series' indicates the ignition position.

In the upper part of Fig. 6 photos of an experiment with inside ignition in position CMS after 4s (case 2, 1.5 g H_2) are shown, where after a circular expansion of the flame kernel close to the ignition position the flame travels upwards and then along the lid before it starts to burn downwards. When the flame front reaches the upper rim of the upper vent opening it propagates to the outside of the enclosure, where the flammable mixture present there is burned. Inside the enclosure no flame or burnt gas was detected below the upper vent opening, so only signals of the uppermost photodiodes can be expected for these experiments. In the record of pressure sensor PT4 that was positioned close to the lid of the enclosure merely a negative temperature shift but no pressure increase was detected. In the

lower part of Fig. 6 BOS-photos of an experiment with outside ignition in position OUT after 4 s (case 1a, 3 g H_2) are depicted. In this experiment the hydrogen containing mixture that had left the enclosure via the upper vent opening was ignited, but the flame did not manage to enter the enclosure. In this case none of the sensor records showed signals of a combustion.

Figure 7 shows the BOS-photographs of an experiment where a combustion was detected in the whole enclosure after a delayed ignition in position CMS (case 2, 4 g H_2). In this experiment the photodiodes produced signals due to the combustion but in the records of the pressure sensors again merely a negative thermal shift of the signals was observed. Pressure waves were only measured in experiments with higher hydrogen amounts or other ignition settings.

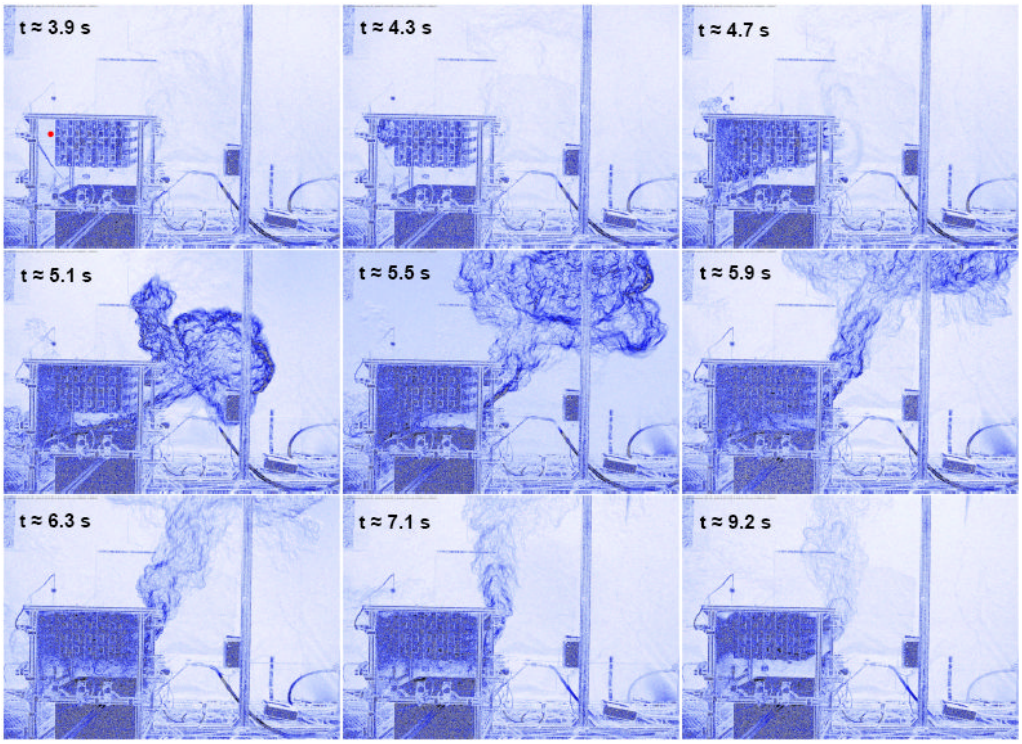

Figure 7: BOS-photos of an experiment with combustion in the whole enclosure after delayed ignition in position CMS (case 2, 4 g H_2) after 4 s. The red dot in the first frame indicates the ignition position.

Using the macroscopic combustion phenomena described above all experiments can be classified in three groups in the test matrix shown in table 2. In this table different colours (and roman numerals) represent different observations during the experiments. Green cells (I) indicate that no combustion or a combustion only in the upper part of the enclosure is detected in the sensor records and in the BOS photos/movies available. If an ignition is detected by the majority of the sensors (pressure sensors merely show a thermal shift of their signals) and in the BOS photos/movies a combustion in the entire volume of the enclosure is observed the corresponding cells are colour-coded yellow (II). Red cells (III) indicate that an ignition is detected in all sensor records (pressure sensors detect pressure waves apart from the thermal shift of their signals), and in the BOS photos/movies a combustion in the entire volume of the enclosure is observed. Table 2 shows that in experiments with a permanent inside ignition stronger combustion phenomena were observed than in experiments with an inside ignition of the same amount of released H_2 after 4 s. For both ignition settings the observed combustion phenomena were similar for the same hydrogen amount, independent of the venting situation (case) investigated in the experiment. Solely the experiment on case 1b with permanent ignition and a released hydrogen amount of 1.5 g shows a weaker burning behaviour than the other experiments with this H_2-amount and these ignition settings. With a delayed outside ignition after 4 s similar combustion

behaviours were observed for the cases 1a, 1b, and 2, while in the experiments on case 3 no ignition of the released H_2 was observed by the sensors even for a released hydrogen amount of 4 g. With a permanent outside ignition the combustion behaviours of the cases 1a, 2, and 3 are similar, while stronger combustions were observed in the experiments on case 1b.

Table 2: Combustion phenomena observed in the experiments (green (I): no or regional combustion, yellow (II): combustion in the entire enclosure but no pressure signals, red (III): combustion in the entire enclosure with pressure signals).

	Scenario C (inside ignition) Case				Scenario D (outside ignition) Case				
H_2-Amount [g]	1a	1b	2	3	1a	1b	2	3 (OUT)	3 (EXT)
Delayed ignition after 4 s for a duration 300 ms									
1.5	I	I	I	I	I	I	I	I	I
3	I	I	I	I	I	I	I	I	I
4	II	II	II	II	II	II	II	I	I
5					III	III	III		
6	III				III	III	III		
14.85							III		
23.41					III				
Permanent ignition for the first 5 s of an experiment									
1.5	II	I	II	II	I	I	I	I	I
3	III	III	III		I	II	I	I	I
4	III				II	III	II	II	II

For the experiments where a flame front was detected by at least two photodiodes of a row, it is possible to calculate flame velocities along this row using the arrival times of the flame front at the lines monitored by the photodiodes. The maximum flame velocities determined via this method are plotted against the released hydrogen amount in the left graph of Fig. 8. The graph shows that the maximum flame velocities increase with increasing hydrogen amount. Furthermore it can be observed that the velocities are higher with a permanent than with a delayed ignition, and they are also higher for an inside ignition than for an outside one. The highest velocities were measured for experiments with a permanent inside ignition, the lowest ones for experiments with outside ignition after 4 s. In the graph the maximum velocities determined for the additional experiments with released H_2-amounts of 14.85 g (533 m/s) and 23.41 g (391 m/s) are omitted to reduce the scale of the abscissa for clarity.

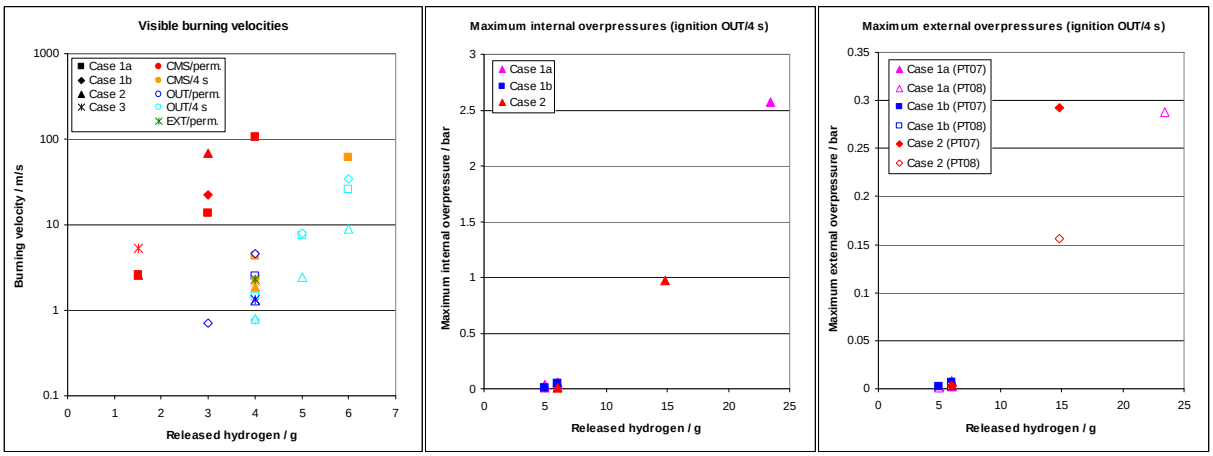

Figure 8: Maximum flame velocities determined from the arrival times of the flame front at the lines monitored by the photodiodes (left) and maximum overpressures measured inside (centre) and outside (right) the enclosure model.

From the combustion phenomena listed in table 2 it can be read that only a small number of experiments allowed determining maximum overpressures of pressure waves generated during the combustion. In the centre graph of Fig. 8 the maximum overpressures measured by one of the inside pressure sensors (PT01-04) is plotted against the released hydrogen amount for the experiments with delayed ignition after 4 s in position OUT, for which a larger number of release rates was investigated than in the experiments with other ignition settings. For the experiments with a released hydrogen amount of up to 6 g maximum overpressures of less than 110 mbar were measured, while in the two additional experiments maximum pressures of almost 1 bar (14.85 g H_2) and more than 2.5 bar (23.41 g H_2) were found. The graph shows that the maximum overpressure measured inside the enclosure increases almost linearly with increasing hydrogen amount. The right graph of Fig. 8 shows the maximum overpressures measured by the second sensor of the outside pressure sensor rows positioned to the left (PT07, solid symbols) and the right (PT08, open symbols) side of the enclosure. The second sensor was chosen since the first sensor on the ignition side (PT06) is most likely already affected with a thermal shift before the pressure wave reaches it. Again the measured overpressures increase almost linearly with increasing hydrogen amount, whereas the slope of the pressure increase of the sensors located at the right (ignition) side of the enclosure is lower than the slope for the pressure increase on the left side of the enclosure. The same behaviour is found for the overpressure values, where higher overpressures were found on the left than on the right (ignition) side of the enclosure. This behaviour is not only due to the lager distance of PT08 to the centre of the upper vent opening (1250 mm) compared to the distance of PT07 to the centre of the lower vent opening (1005 mm), since the overpressure values measured by the farthest sensor to the left of the enclosure (PT09, 1504 mm) are still considerably higher than the ones measured by PT08.

An analysis of different studies on the effects of pressure waves on human beings was published by Richmond et al. in 1986 [1]. The results of this analysis are summarized in the left part of Fig. 9 where the maximum overpressure (positive amplitude) in Pa is plotted against the duration of the positive overpressure in ms. The solid symbols added to this diagram represent the maximum overpressures measured inside the enclosure during the experiments with their corresponding positive amplitude duration. The colour of the dots indicates the configuration of the enclosure model (case), while the shape and the number besides the dots give the ignition settings and the released hydrogen amount.

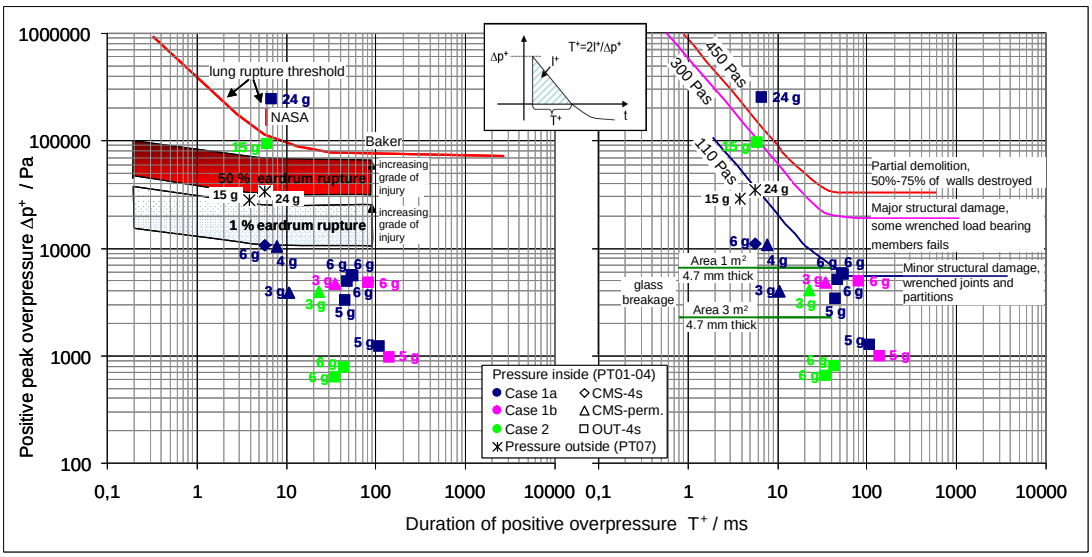

Figure 9: Possible effects of overpressure waves on human beings (left) [1] and building structures (right) [2] with added data points of the maximum overpressures measured during the experiments.

As can be seen from the left graph, the two additional experiments with released hydrogen amounts of approx. 15 and 24 g lie above the region where ear drum ruptures occur with a probability of 50%.

Even lung ruptures may be possible in the experiment with an H_2-inventory of 24 g. Two further experiments with hydrogen amounts of 6 g (case 1a, CMS/4s) and 4 g (case 1a, CMS/perm.) reach the region in the diagram where ear drum ruptures may occur with a limited probability. The data points of the other experiments where overpressures could be determined lie below the regions where human beings may suffer injuries, but all square symbols represent experiments with outside ignition after 4 s, which is the ignition setting where the lowest flame velocities were achieved for a given hydrogen amount compared to the experiments with other ignition times and positions. In the right graph of Fig. 9 the maximum pressures and positive amplitude durations measured inside the enclosure were added (solid symbols) to a graph summarizing possible damages to building structures due to pressure waves [2]. As the graph shows, the loads generated in the experiments with 15 and 24 g H_2 lie in the region where major structural damage has to be expected. The majority of the remaining data points lie in the region where glass breakage of smaller windows (area: 1 m^2) and minor structural damage is possible.

Using the maximum overpressures determined from the signals of pressure sensor PT07, which was located in a distance of approx. 1 m to the centre of the lower vent opening, a similar estimation of the possible injuries can be performed, but in this case only in the two additional experiments (15 and 24 g H_2) pressure waves causing ear drum ruptures with a considerable probability were measured. These two data points are added as stars to the diagrams depicted in Fig. 9 although in the experiment with 24 g H_2 the measuring range for PT07 was exceeded, so in reality this data point is located at an even higher overpressure. All other experiments where pressure waves were detected by this sensor produced signals well below the regions in the diagram that indicate injuries to human beings. In a distance of 1 m to the lower vent opening still minor structural damage and glass breakage of small windows is possible for the additional experiments. In the experiments with hydrogen amounts of up to 6 g overpressures below the line indicating glass breakage of larger window glasses (area: 3 m^2) were measured, but again in most of the experiments the ignition settings producing the lowest flame velocities (OUT/4s) were used, so with inside or permanent ignition higher loads have to be expected for the same released hydrogen amount.

4.0 SUMMARY AND CONCLUSIONS

In more than 200 experiments the hazard potential of a severe hydrogen leakage inside a fuel cell cabinet was investigated using a generic fuel cell enclosure model with an internal volume of approx. 560 l. In all experiments 120 l of this total volume were blocked by a solid cube representing large internals of the fuel cell, small internals were simulated by grid obstacles blocking different amounts of the internal enclosure volume in two internal geometries investigated. Based on the description of a commercially available fuel cell unit the maximum hydrogen release rate possible in the case of a rupture of the hydrogen feed line inside the enclosure was evaluated to 15 g H_2/s, so in the experiments hydrogen release rates from 1.5 to 15 g H_2/s were used. A security mechanism, based on the pressure decrease inside the hydrogen lines of the fuel cell after the rupture of the feed line was assumed to shut down the H_2-supply after 1 s. With this assumption and the release rates evaluated three cases with different venting characteristics of the enclosure model were investigated.

The experimental work started with distribution experiments, where H_2-concentrations were determined in selected positions in- and outside the enclosure model during fixed time periods after the release. Additionally the distribution behaviour of the injected hydrogen was monitored using the BOS technique, an optical method for the visualisation of density gradients. In the combustion experiments two scenarios differed by the location of the ignition point were investigated. In scenario C one ignition position inside the enclosure was used, while in scenario D two positions outside the enclosure were investigated. Two ignition times were used in the experiments.

From the results of the experiments the following conclusions can be drawn:

Enclosure obstruction: In contrast to the experiments with low obstruction, with the highly obstructed internal geometry a chimney effect inside the enclosure was not observed, leading to very high

hydrogen concentrations inside the model. Another reason for the high H_2-concentrations in this internal geometry is the partial blocking of the vent openings by the grid obstacles. Compacting these obstacles would allow avoiding an obstruction of the vent openings and would furthermore minimise the hazard of possible flame acceleration in distributed obstructed areas.

Venting: The number and arrangement of the vent openings used in the experiments enabled the appearance of a chimney effect inside the enclosure. The three main venting characteristics investigated showed little difference between the maximum H_2-concentrations measured during the experiments; however differences in the H_2-transport to the outside of the enclosure and in the homogeneity of the H_2-distribution were recognised. In the cases 1a and 2 an inhomogeneous hydrogen distribution inside the enclosure and a rather slow transport to the outside was observed, while in the cases 1b and 3 a more homogeneous H_2-distribution and a faster transport to the outside was reached. In the combustion experiments the two cases 1a and 2 generated similar loads, but different combustion behaviours were found in some of the experiments on the cases 1b and 3: The active venting used in case 1b is responsible for a comparably slow combustion with a released hydrogen amount of 1.5 g for permanent inside ignition. In this experiment similar transport ratios of hydrogen release and fan induced flow were reached. With the higher hydrogen amount of 3 g the flame velocities determined inside the enclosure model were similar to the ones of the corresponding experiments on the cases 1a and 2. The opposite effect of the active venting was found in experiments with permanent outside ignitions, where stronger combustions were observed for released hydrogen amounts of 3 and 4 g H_2 compared to the other cases. For delayed ignitions similar combustion behaviours as in the other cases were observed. In the experiments on case 3 an effect of the additional chimney was observed with delayed outside ignition, where even released hydrogen amounts of 4 g did not cause any detectable pressure wave. For the other ignition settings similar burning behaviours as in the other cases investigated were observed.

Ignition position and time: In combustion experiments with the same hydrogen amount a permanent ignition generated higher loads than a delayed one, and also an inside ignition produced stronger combustions than an outside one. The highest loads were detected with a permanent inside ignition, while the slowest combustions were observed for delayed outside ignition.

Hydrogen amount: The highest combustion loads for a given amount of released hydrogen were observed in the experiments with permanent inside ignition. With these ignition settings a combustion was detected by all the sensors even in experiments with a H_2-amount of 1.5 g. The ignition of 3 g H_2 resulted in pressure waves with a maximum amplitude of 40 mbar inside the enclosure model; such pressure loads can cause glass breakage of large windows. In the experiment with 4 g H_2 and permanent inside ignition pressure waves with a maximum amplitude of circa 100 mbar were observed inside the enclosure, that may even injure human beings. Although the enclosure model survived this test, other enclosure types may well be damaged, or missiles may be generated during the explosion.

The findings of the experiments demonstrate that for the diminishing of possible hazards it is necessary to reduce the hydrogen amount that can be released from a ruptured pipe inside the fuel cell enclosure by constructional means to below 1.5 g. In the distribution experiments with this release rate hydrogen concentrations only slightly above the flammability level for H_2/air-mixtures were found in the low obstructed internal geometry. In most of the combustion experiments with this hydrogen amount no combustion was observed, and even with the ignition settings producing the highest combustion loads no dangerous pressure waves were detected inside the enclosure.

5.0 REFERENCES

1. Richmond, D.R., Fletcher, E.R., Yelverton, J.T. and Phillips, Y.Y., Physical correlates of eardrum rupture, *Ann. Otol. Rhinol. Laryngol.*, **98**, 1989, pp. 35–41.
2. Baker, W. E., Cox, P. A., Westine, P. S., Kulesz, J. J., and Strehlow, R. A., Explosion Hazards and Evaluation, 1983, Elsevier Scientific Publishing Co., Amsterdam, The Netherlands.